

Oxygen-content-dependent electronic structures of electron-doped cupratesDongjoon Song,¹ Seung Ryong Park,^{1,*} Chul Kim,¹ Yeongkwan Kim,¹ Choonsik Leem,¹ Sungkyun Choi,^{1,†} Wonsig Jung,¹ Yoonyoung Koh,¹ Garam Han,¹ Yoshiyuki Yoshida,² Hiroshi Eisaki,² D. H. Lu,³ Z.-X. Shen,³ and Changyoung Kim^{1,‡}¹*Institute of Physics and Applied Physics, Yonsei University, Seoul 120-749, Korea*²*National Institute of Advanced Industrial Science and Technology, Tsukuba 305-8568, Japan*³*Department of Physics, Department of Applied Physics, and Stanford Synchrotron Radiation Laboratory, Stanford University, Stanford, California 94305, USA*

(Received 9 August 2012; revised manuscript received 5 October 2012; published 17 October 2012)

We performed systematic angle-resolved photoemission studies on as-grown and oxygen-reduced electron-doped cuprates $\text{Pr}_{0.85}\text{LaCe}_{0.15}\text{CuO}_4$, $\text{Nd}_{1.85}\text{Ce}_{0.15}\text{CuO}_4$, and $\text{Sm}_{1.85}\text{Ce}_{0.15}\text{CuO}_4$, in order to investigate the oxygen-reduction process. All of the as-grown systems we have studied show metallic edges in the antinodal region, while near E_F nodal spectra are suppressed, resulting in partial gap opening. In addition, spectra from as-grown systems show weak and broad low-energy quasiparticle peaks (QPPs). Upon proper reduction, sharp QPPs emerge but they are strongly suppressed again in the over-reduced state. This QPP behavior deviates from the magnetism and doping-evolution origin of QPP suppression, and implies that scattering due to disorder and impurity is a more probable cause for the broken coherence of the quasiparticle state. Our results are also consistent with the recently proposed Cu-deficiency scenario.

DOI: [10.1103/PhysRevB.86.144520](https://doi.org/10.1103/PhysRevB.86.144520)

PACS number(s): 74.25.Jb, 74.72.Ek, 75.50.Ee, 74.62.En

I. INTRODUCTION

Cuprate high-temperature superconductivity is induced when carriers are introduced into copper oxide planes in insulating mother compounds. However, for electron-doped cuprates, $R_{2-x}\text{Ce}_x\text{CuO}_4$ ($R = \text{La, Pr, Nd, Sm, Eu, Gd}$), an additional annealing process in a low-oxygen environment is required to induce superconductivity. The process is supposed to reduce the oxygen content.^{1,2} Exactly what happens during the reduction process has not been clearly settled. It was initially believed that the annealing process removes extra intersite apical oxygen.¹ However, it was recently argued that oxygen is mainly removed from in-plane oxygen sites,^{3,4} which means that as-grown crystals have Cu deficiencies.^{5,6}

Meanwhile, how the reduction process affects various physical properties is another issue. For instance, the reduction process is known to affect transport properties, optical responses, and magnetism in addition to superconductivity.^{1-4,7-12} For this reason, electronic structures have been studied, especially by means of angle-resolved photoemission spectroscopy (ARPES), to investigate the effect of the reduction process. It was reported that a shadow band exists in as-grown samples due to a strong antiferromagnetic (AF) renormalization effect and that it disappears in reduced samples.¹³ A consistent result was also obtained from an AF tight-binding fit of the measured electronic structure.¹⁴ These results suggest that the reduction process destroys the AF order, which appears to be consistent with neutron scattering results.^{9,10} In addition, many of the physical properties of the optimally doped as-grown state, including the AF order, are similar to those of an underdoped state. It was thus believed that the reduction process increases the electron doping.⁸

However, there are still several issues to be resolved. While the ARPES result from as-grown $\text{Pr}_{1.85}\text{Ce}_{0.15}\text{CuO}_4$ (PCCO) shows a gap over the entire Fermi surface,¹³ as-grown $\text{Nd}_{1.85}\text{Ce}_{0.15}\text{CuO}_4$ (NCCO) shows a gap only around the nodal region.¹⁴ It is here stressed that the gap does not refer to the superconducting gap but to a normal-state gap or suppression

of the spectral weight near the Fermi energy. Whether there indeed is a rare-earth-element dependence in the low-energy electronic structure needs to be resolved. Moreover, it has been pointed out that there is a quantitative mismatch between the effective doping from the reduction and the actual underdoping required to account for the measured physical properties.^{7,15} That is, the doping effect alone may not be enough to explain the change associated with the reduction process. In spite of these issues, what additional factors are needed and/or how Cu deficiency may affect the electronic structure do not appear to have been addressed in previous studies.

To resolve these issues, we performed ARPES studies on differently oxygenated electron-doped cuprates with various rare-earth elements, $\text{Pr}_{0.85}\text{LaCe}_{0.15}\text{CuO}_4$ (PLCCO), NCCO, and $\text{Sm}_{1.85}\text{Ce}_{0.15}\text{CuO}_4$ (SCCO). Whether there is a universal feature or not in the low-energy electronic structure of as-grown electron-doped cuprates can be addressed through a systematic study of the rare-earth dependence. As for the issue of the doping effect in the reduction mechanism, we performed ARPES studies not only on as-grown and reduced samples but also on over-reduced samples.⁶ Study of the over-reduced state provides an opportunity to discern the doping and disorder effects, as will be discussed later. We try to interpret the experimental results on low-energy electronic structures within the Cu-deficiency scenario.

II. EXPERIMENT

PLCCO, NCCO, and SCCO single crystals were grown by the traveling-solvent floating-zone method. All the crystal rods were cleaved into small pieces and annealed in high-purity N_2 for 10–24 h at 900–950 °C and in O_2 atmosphere for 5–20 h at 500 °C. The T_c 's of PLCCO, NCCO, and SCCO were 22, 24, and 19 K, respectively. To make over-reduced PLCCO, optimally reduced superconducting PLCCO was annealed at 930 °C in N_2 again. We did not quench the over-reduced sample to prevent T_c relaxation during the cool down.⁶ We performed

ARPES experiments at the beamline 5-4 of the Stanford Synchrotron Radiation Light source. Samples were cleaved *in situ* and experiments were performed at temperatures below 30 K, in a pressure better than 4×10^{-11} Torr. We used 16.5 eV photons with 14 meV overall energy resolution. Even though ARPES spectra were taken only with 16.5 eV photon (thus a fixed k_z), our data are expected to represent the electronic structure for all k_z . This is because the band structures measured with other photon energies show very little, if any, k_z dependence.^{16,17}

III. RESULT AND DISCUSSION

A. Gap in as-grown systems

We first discuss the normal-state gap issue. Figure 1(a) shows Fermi surface (FS) maps of as-grown and reduced NCCO and SCCO, constructed by integrating an energy window of ± 12.5 meV around the Fermi level. Glancing at the FS maps of as-grown samples (left figures), we see that there is no spectral weight crossing the Fermi level (E_F) around the nodal region in strong contrast to the reduced case [right panels of Fig. 1(a)]. A consistent behavior can be also seen in the nodal band ARPES images in Fig. 1(b). A gaplike feature is

observed in the as-grown spectrum while the band crosses the Fermi level in the reduced spectrum. The nodal band gap can be most clearly seen in the energy distribution curve (EDC) at the Fermi momentum (k_F) shown in Fig. 1(c). A fully opened gap with a ~ 20 meV leading-edge shift (LES) is observed in as-grown samples while it is absent in reduced samples. A notable aspect of the spectra from reduced SCCO is that the nodal gap is not fully closed either. This aspect will be discussed in the following section. Here we point out that the small superconducting gap of ~ 2 meV does not affect our discussion as it is much smaller than the energy resolution and scale we discuss.¹⁸

Band gap opening and closing in the nodal region for as-grown and reduced electron-doped cuprates have been reported for the PCCO and NCCO systems.^{13,14} In the reports, it was suggested that the gap opens due to the strong AF effect in the as-grown system. Based on simulation results, it was argued that a 20 meV nodal band gap may open when the hot-spot gap is larger than 60 meV.¹³ In our result in Fig. 1(d), the hot-spot gap is larger than 60 meV for both NCCO and SCCO. It thus suggests that the nodal band gap in the as-grown system can be the result of a strong AF effect. This is also supported by the observation that the in-gap spectral weight at the hot spot is higher for the reduced compared to the as-grown compound, as seen in Fig. 1(d). Since the in-gap spectral weight at the hot spot anticorrelates with the AF correlation length,¹⁹ it is natural to assume that the reduction process destroys the AF order and closes the nodal gap.

Despite the consistent behavior of the gaps of PCCO, NCCO, and SCCO in nodal and hot-spot regions, the antinodal gap behavior for as-grown systems remains an issue. A 20 meV LES in the antinodal region was observed in as-grown PCCO,¹³ but not in as-grown NCCO.¹⁴ A quick look at our antinodal region data plotted in Figs. 2(a) and 2(b) shows no sign of a gap feature. In order to have a more careful look, we plot normalized antinodal EDCs of as-grown and reduced NCCO in Fig. 2(c). It can be clearly seen that the leading edges of the two NCCO spectra coincide very well. As for the SCCO case, the spectra were not measured at the same temperature and thus comparison of them may not be as direct. However, we can still compare the leading-edge midpoints after we scale the EDCs so that they have the same height. It is seen that the midpoints of the leading edges coincide very well, suggesting that there is no gap. Moreover, the leading edge of the as-grown SCCO matches that of a gold spectrum taken at the same temperature. All these results show that the antinodal gap is absent for both as-grown and reduced NCCO and SCCO.

We also studied the reduction effect in PLCCO, and our PLCCO data show a consistent gap behavior. The antinodal spectra of as-grown and reduced PLCCO plotted in Fig. 3(b) have the same peak energy (filled green triangle), and their leading edges coincide with the gold Fermi edge. That is, no antinodal gap is observed for as-grown PLCCO. Meanwhile, the nodal band spectrum of as-grown PLCCO in Fig. 3(c) shows a fully opened gap. Summarizing our experimental observations of the gap behavior in as-grown samples, all of the compounds NCCO, SCCO and PLCCO as grown show partially open gaps along the Fermi surface (a gap in the nodal region but a metallic edge in the antinodal region).

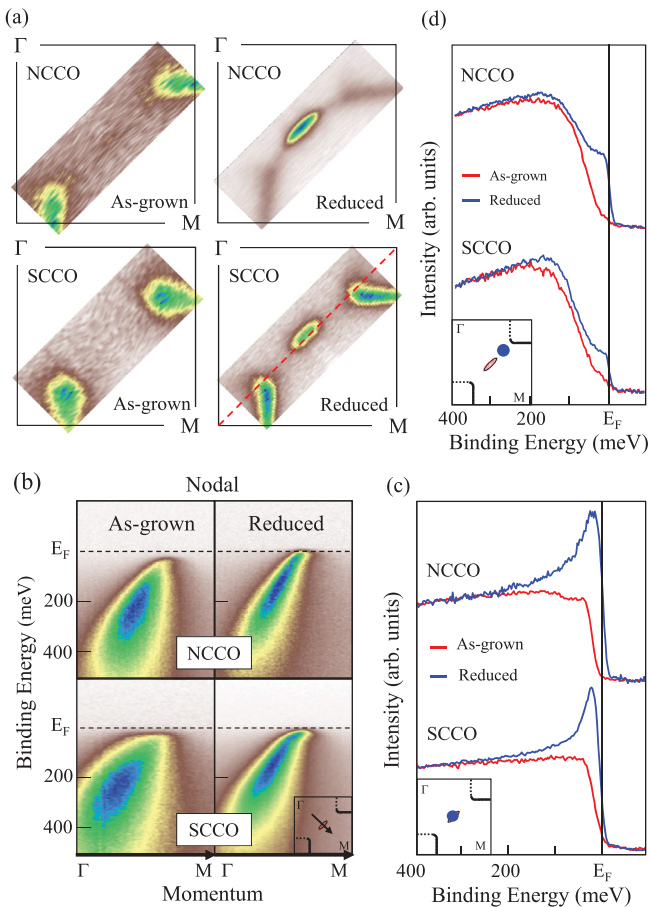


FIG. 1. (Color online) (a) Fermi surface maps of as-grown and reduced NCCO and SCCO. The red dotted line in the right bottom panel represents the AF zone boundary. (b) ARPES data along the nodal cut. (c) EDCs from the nodal point, marked in the inset as a blue dot. (d) EDCs from the hot spot as marked in the inset.

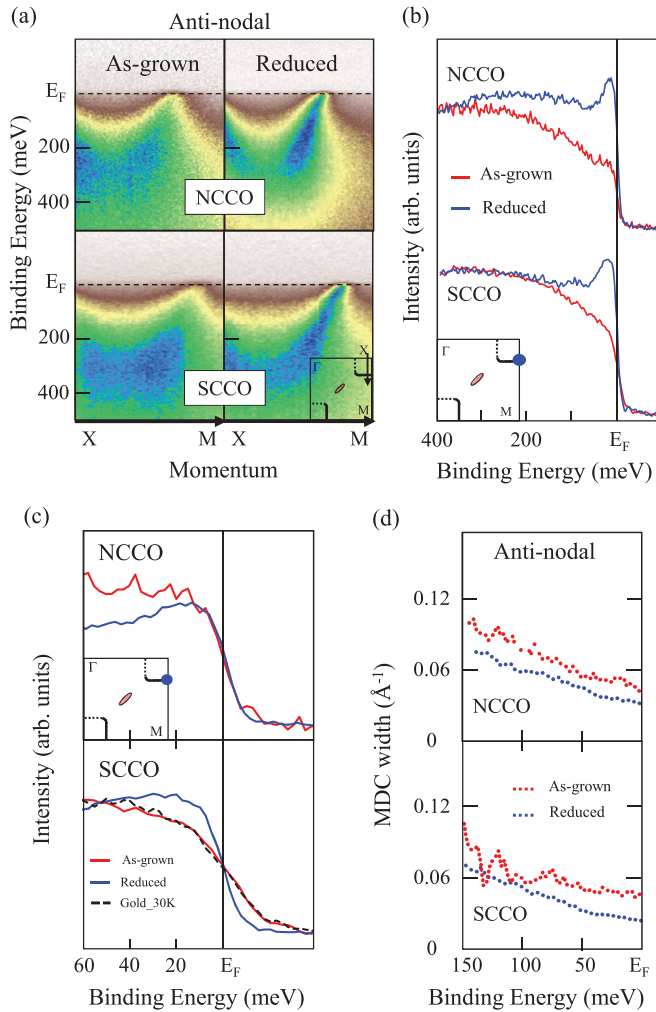


FIG. 2. (Color online) (a) As-grown and reduced antinodal data from NCCO and SCCO. (b) EDCs at the antinodal point of as-grown and reduced NCCO measured at 15 K. (c) Antinodal EDCs of as-grown (measured at 30 K, red solid line) and reduced (measured at 10 K, blue solid line) SCCO. The yellow dotted line in (c) is a gold spectrum measured at 30 K. (d) MDC widths of NCCO and SCCO antinodal bands as a function of energy.

We wish to point out that this partially gapped FS (only around the nodal region) for as-grown electron-doped cuprates agrees with previous Hall measurements. It has been reported that R_H from an overdoped as-grown $\text{Pr}_2\text{Ce}_{2-x}\text{CuO}_4$ thin film shows a similar temperature dependence to that of an underdoped reduced system. However, R_H for the overdoped as-grown case was found to be much smaller than that of the underdoped reduced system. In fact, as far as the magnitude goes, the overdoped as-grown case was rather similar to the overdoped reduced material.⁷ Such observations were understood to indicate that, upon reduction, the electron carrier number stays more or less the same while the hole carrier number changes significantly. The authors thus suggested that hole pockets in the nodal region appear upon reduction. Our ARPES results also show that the nodal hole pocket is missing in all of the as-grown samples, consistent with the interpretation of the authors of Ref. 7. Even though we have not studied PCCO, a similar AF effect on the

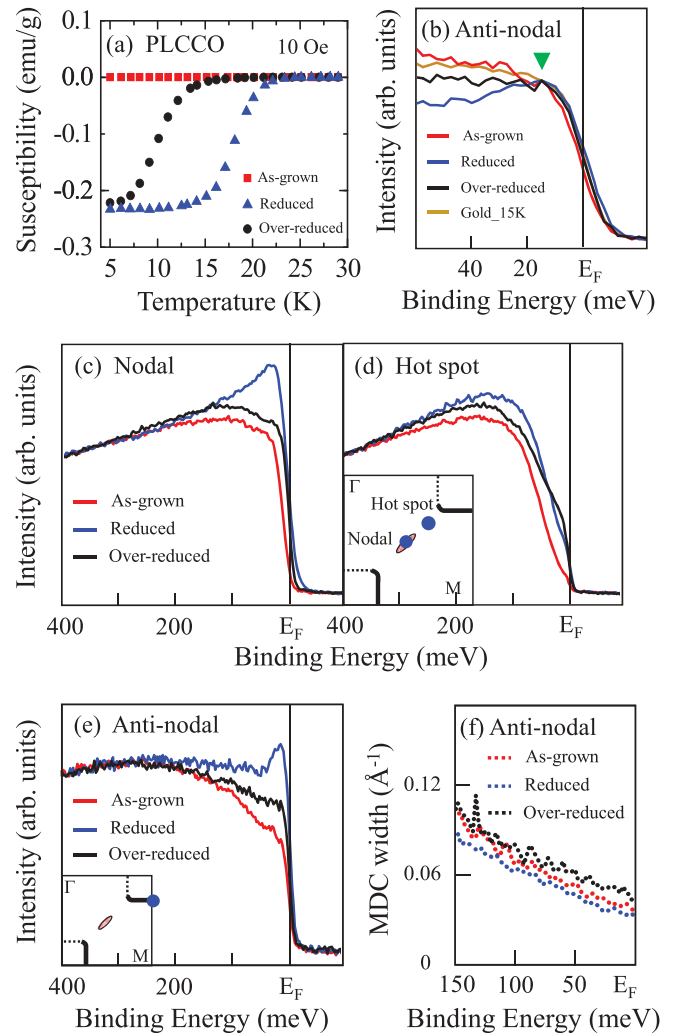


FIG. 3. (Color online) (a) Magnetic susceptibility of as-grown, reduced, and over-reduced PLCCO. (b) EDC at the antinodal point. Black solid line corresponds to the gold EDC. (c),(d) EDCs of PLCCO at the nodal point and hot spot, respectively. (e) Same as (b) but with a different energy scale. (f) Antinodal band MDC widths. All the spectra were measured at 15 K.

electronic structure has been reported for optimally doped PCCO ($x = 0.15$).²⁰

B. Disorder and impurity effects on low-energy quasiparticle states

We now turn our attention to quasiparticle states. We try in particular to explain the quasiparticle peak (QPP) behavior in terms of disorder and impurity (DI) scattering. In the nodal and antinodal EDC plots in Figs. 1(c) and 2(b), a QPP is observed in the reduced samples but not in the as-grown ones. This QPP evolution as a function of reduction is regarded as an isotropic phenomenon because it is observed over the entire FS (except in the hot-spot area where the strong AF renormalization effect inhibits development of a QPP even for the reduced system). In other words, isotropic QPP suppression happens only in as-grown samples. Such an isotropic low-energy QPP suppression in the ARPES result leads us to believe that it is from a local effect such as DI scattering.

For instance, ARPES studies^{21,22} on Zn-doped $\text{La}_{2-x}\text{Sr}_x\text{CuO}_4$ (LSCO) and hydrogen-dosed graphene²³ report an isotropic QPP suppression due to impurity scattering. Likewise, the QPP suppression in as-grown NCCO and SCCO can also be attributed to the DI scattering effect.

If the suppression of the QPP is indeed caused by the DI scattering, it will also be accompanied by peak broadening. Since the nodal band of the as-grown system has a fully opened gap, comparing its bandwidth to that of the reduced system may not be reliable. On the other hand, the antinodal band of the as-grown system does not have such a gap issue and we can thus compare the peak widths of as-grown and reduced systems. Figure 2(d) plots momentum distribution curve (MDC) widths of the antinodal band. It is seen that the MDC widths of as-grown samples are larger than those of reduced samples. This low-energy peak broadening along with the QPP suppression is consistent with the idea that DI scattering exists in the CuO_2 plane for the as-grown system, while the reduced system has relatively clean and homogeneous planes.

However, it should be noted that the QPP suppression mechanism can be understood in a different way. Since QPP enhancement in the reduced system occurs simultaneously with destruction of the AF order, the AF renormalization effect can also be suspected as the origin of QPP evolution. However, there are two reasons why we believe this is not the case. First, the antinodal band of the as-grown sample shows suppressed and broadened QPPs even though it is located far from the AF zone boundary. Second, there still is a fairly strong AF band renormalization effect even in the reduced system as evidenced by the small nodal gap of ~ 5 meV and trivial gap filling at the hot spot [see Figs. 1(c) and 1(d)].^{16,24} Nevertheless, reduced SCCO has sharp QPPs. In this regard, the QPP evolution does not appear to be strongly correlated with the AF order.

C. Quasiparticle suppression in over-reduced PLCCO

Even though there are reasons to believe that QPP evolution is not driven by the AF order strength but by DI scattering, we can go further to settle the issue. The difficulty in resolving the issue comes from the fact that oxygen reduction is accompanied by enhancement of QPPs and electron doping at the same time, raising the possibility that the extra doping from the reduction weakens the AF order and thus enhances the QPPs. A way to overcome this problem is to study over-reduced samples. According to a recent oxygen-content-dependent superconducting transition study on $\text{Pr}_{0.88}\text{LaCe}_{0.12}\text{CuO}_4$, T_c decreases when the amount of removed oxygen exceeds the optimum value.⁶ It was also suggested that the over-reduced state contains sufficient DI. That is, the over-reduced state is effectively located in the more overdoped region, yet has more DI than the optimally reduced state. Comparison of the QPP features of as-grown, reduced, and over-reduced PLCCO provides an opportunity to discern the doping and DI effects.

Figure 3(a) shows magnetic susceptibility curves for as-grown, reduced, and over-reduced PLCCO. Over-reduced PLCCO has a T_c more than 5 K lower than that of the reduced sample. The process from the reduced to the over-reduced state or the other way is reversible through annealing at 500 °C

in air or oxygen. That is, the over-reduction process affects the oxygen content only and does not appear to severely change the crystal structure. This situation is also found in $\text{YBa}_2\text{Cu}_3\text{O}_{7-\delta}$ (YBCO) for which the oxygen content can be controlled through 500 °C oxygen annealing. In addition, the superconducting volume remains the same for reduced and over-reduced samples. This shows that the lower T_c of the over-reduced state is a bulk property.

From the ARPES results in Fig. 3(b), we note that the PLCCO data show no antinodal band gap, as discussed earlier. Moreover, the results show that the nodal gap progressively closes and the in-gap spectral weight gradually grows in the nodal and hot-spot regions when PLCCO is oxygen reduced from as grown to over-reduced. These observations upon oxygen reduction are consistent with the results from other electron-doped cuprates, and reflect the fact that AF order becomes weaker upon oxygen reduction. However, the QPP behavior deviates from this tendency. Looking at the data in Figs. 3(c) and 3(e), we see that the QPP is enhanced as we go from as grown to reduced. However, as we further reduce PLCCO to the over-reduced state, the QPP disappears again over the entire FS as shown in Figs. 3(c), 3(d), and 3(e). In addition, the MDC width of the antinodal band in Fig. 3(f) shows that the over-reduced sample has the broadest peak among the three cases.

There are three possible factors that can affect the oxygen-content-dependent QPP behavior of PLCCO from the as-grown to the over-reduced state: (i) weakened AF order, (ii) simple doping effect, and (iii) DI scattering. Among these, weakening of AF order is likely to couple to the doping effect because the electron doping in the reduction process (removal of an oxygen anion) should progressively reduce the AF order, as is experimentally observed. If the QPP enhancement upon oxygen reduction were caused by the weakened AF order, we would have observed even sharper QPPs for the over-reduced system for which AF order is the weakest. However, the QPP is the strongest in the optimal state. This QPP tendency distinct from AF order indicates that coherence of the quasiparticle state has no significant correlation with the weakened AF order or doping effect. Since (i) and (ii) are ruled out, it is likely that (iii) DI scattering is the major cause for the overall QPP behavior. Accordingly, the optimally reduced PLCCO has the cleanest and most homogeneous CuO_2 plane with coherent QPPs while the others contain some DIs which cause QPP suppression and broadening.

D. Implication for oxygen-reduction mechanism

Identification of the DI scattering as the main cause of the QPP suppression has an implication for the oxygen-reduction mechanism. There are three oxygen sites in the T' structure of electron-doped cuprates: out-of-plane, apical, and in-plane sites. We first consider the removal process from the as-grown to the reduced state. According to previous optical measurements^{3,4} and neutron scattering and thermogravimetric analysis,⁵ out-of-plane oxygen atoms are scarcely removed in the reduction process. Even if some of these oxygen atoms are removed, the overall effect on the QPP suppression is expected to be very weak because the site is located far from CuO_2 planes. For the apical oxygen site, removal of

randomly distributed extra oxygen atoms at apical sites may naturally explain the QPP enhancement. Nevertheless, it is difficult to imagine that the small amount of apical oxygen (less than 2% oxygen away from the CuO_2 plane) alone can suppress the QPPs as drastically as shown in our data for the as-grown systems. On the other hand, in the Cu-deficiency scenario in which in-plane oxygen atoms are removed,^{5,6} QPPs are expected to be suppressed in the as-grown state as the Cu-deficiency defects are in the CuO_2 planes. As defects in CuO_2 planes are repaired through reduction, QPPs can be enhanced in the reduced state.

Upon further reduction, more oxygen atoms are removed from either in-plane or apical sites. The observation of drastic QPP suppression in our over-reduced ARPES data again suggests that oxygen atoms are removed from in-plane sites in the over-reduced system because in-plane oxygen vacancies are expected to be strong scatterers while removal of the remaining apical oxygen atoms only reduces the DI effect. It is also natural to expect that more in-plane oxygen atoms are removed upon further reduction into the over-reduced state, since in-plane oxygen atoms are also removed in the initial reduction process in the Cu-deficiency scenario. In fact, the in-plane oxygen removal picture has already been suggested to explain the over-reduced state of PLCCO.⁶ Therefore, our ARPES data and other experimental results consistently suggest that oxygen atoms are removed from in-plane sites through reduction processes.

While the quasiparticle dynamics can be mostly understood within the DI scattering scenario, DI scattering alone may not explain why superconductivity disappears in the as-grown state. According to the data in Figs. 3(a) and 3(f), over-reduced PLCCO still shows superconductivity even though it has a broader MDC than the as-grown sample. Since the MDC width is related to the scattering rate, it appears that quasiparticles in over-reduced PLCCO are more strongly scattered than those in as-grown PLCCO. If the DI scattering is the major factor in the suppression of superconductivity, one would not expect

superconductivity in over-reduced PLCCO as in as-grown PLCCO. One possible solution to this problem is that the stronger AF order caused by Cu deficiencies in the as-grown state plays an important role. The character rather than the number of impurities could also be important. To resolve this issue, further studies on DI effects are needed.

IV. CONCLUSION

In summary, we have investigated, through systematic ARPES studies, the oxygen-reduction mechanism in electron-doped cuprates. Concerning the controversial gap issue in the as-grown state, a fully opened gap exists near the nodal area but metallic edges are observed in the antinodal region for as-grown NCCO, SCCO, and PLCCO. Upon reduction, progressive gap closing and in-gap spectral weight filling occur in the nodal and hot-spot regions. The gap evolution is a fingerprint of destroyed AF order. We touched upon the Cu-deficiency issue by means of a low-energy QPP study. The reduced samples show coherent sharp QPPs while strongly suppressed and broadened QPPs are observed in as-grown and over-reduced systems, which is evidence for a DI scattering origin of QPP suppression. This is consistent with the Cu-deficiency scenario and supports the in-plane oxygen removal picture. These results suggest that DI scattering is a major factor in the change in quasiparticle scattering through the oxygen-reduction process. However, we also note that DI scattering alone is not enough to account for the disappearance of the superconductivity in the as-grown state.

ACKNOWLEDGMENTS

This work is supported by KICOS Grant No. K20602000008 and under a grant from A3 Foresight program through the NRF of Korea funded by MEST. We also acknowledge support through the BK21 Project. SSRF is operated by the DOE's Office of BES.

*Present address: Department of Physics, University of Colorado at Boulder, Boulder, Colorado 80309, USA.

†Present address: Clarendon Laboratory, University of Oxford, Parks Road, Oxford OX1 3PU, United Kingdom.

‡changyoung@yonsei.ac.kr

¹Wu Jiang, J. L. Peng, Z. Y. Li, and R. L. Greene, *Phys. Rev. B* **47**, 8151 (1993).

²X. Q. Xu, S. N. Mao, Wu Jiang, J. L. Peng, and R. L. Greene, *Phys. Rev. B* **53**, 0871 (1996).

³P. Richard, G. Riou, I. Hetel, S. Jandl, M. Poirier, and P. Fournier, *Phys. Rev. B* **70**, 064513 (2004).

⁴G. Riou, P. Richard, S. Jandl, M. Poirier, P. Fournier, V. Nekvasil, S. N. Barilo, and L. A. Kurnevich, *Phys. Rev. B* **69**, 024511 (2004).

⁵Hye Jung Kang, Pengcheng Dai, Branton J. Campbell, Peter J. Chupas, Stephan Rosenkranz, Peter L. Lee, Qingzhen Huang, Shiliang Li, Seiki Komiyama, and Yoichi Ando, *Nat. Mater.* **6**, 224 (2007).

⁶Yong-Lei Wang, Yan Huang, Lei Shan, S. L. Li, Pengcheng Dai, Cong Ren, and Hai-Hu Wen, *Phys. Rev. B* **80**, 094513 (2009).

⁷J. Gauthier, S. Gagne, J. Renaud, M.-E. Gosselin, P. Fournier, and P. Richard, *Phys. Rev. B* **75**, 024424 (2007).

⁸T. Arima, Y. Tokura, and S. Uchida, *Phys. Rev. B* **48**, 6597 (1993).

⁹H. J. Kang, Pengcheng Dai, H. A. Mook, D. N. Argyriou, V. Sikolenko, J. W. Lynn, Y. Kurita, Seiki Komiyama, and Yoichi Ando, *Phys. Rev. B* **71**, 214512 (2005).

¹⁰S. Kuroshima, M. Fujita, T. Uefuji, M. Matsuda, and K. Yamada, *Physica C* **392–396**, 216 (2003).

¹¹P. Richard, M. Poirier, S. Jandl, and P. Fournier, *Phys. Rev. B* **72**, 184514 (2005).

¹²Shilian Li, Songxue Chi, Jun Zhao, H.-H. Wen, M. B. Stone, J. W. Lynn, and Pengcheng Dai, *Phys. Rev. B* **78**, 014520 (2008).

¹³P. Richard, M. Neupane, Y.-M. Xu, P. Fournier, S. Li, Pengcheng Dai, Z. Wang, and H. Ding, *Phys. Rev. Lett.* **99**, 157002 (2007).

¹⁴M. Ikeda, T. Yoshida, A. Fujimori, M. Kubota, K. Ono, Y. Jaga, T. Sasagawa, and H. Takagi, *J. Phys.: Conf. Ser.* **108**, 012016 (2008).

¹⁵Y. Tanaka, T. Motohashi, M. Karppinen, and H. Yamauchi, *J. Solid State Chem.* **181**, 365 (2008).

- ¹⁶S. R. Park, Y. S. Roh, Y. K. Yoon, C. S. Leem, J. H. Kim, B. J. Kim, H. Koh, H. Eisaki, N. P. Armitage, and C. Kim, *Phys. Rev. B* **75**, 060501(R) (2007).
- ¹⁷N. P. Armitage, D. H. Lu, C. Kim, A. Damascelli, K. M. Shen, F. Ronning, D. L. Feng, P. Bogdanov, Z.-X. Shen, Y. Onose, Y. Taguchi, Y. Tokura, P. K. Mang, N. Kaneko, and M. Greven, *Phys. Rev. Lett.* **87**, 147003 (2001).
- ¹⁸H. Matsui, K. Terashima, T. Sato, T. Takahashi, M. Fujita, and K. Yamada, *Phys. Rev. Lett.* **95**, 017003 (2005).
- ¹⁹H. Matsui, T. Takahashi, T. Sato, K. Terashima, H. Ding, T. Uefuji, and K. Yamada, *Phys. Rev. B* **75**, 224514 (2007).
- ²⁰I. A. Nekrasov, N. S. Pavlov, E. Z. Kuchinskii, M. V. Sadovskii, Z. V. Pchelkina, V. B. Zabolotnyy, J. Geck, B. Buchner, S. V. Borisenko, D. S. Inosov, A. A. Kordyuk, M. Lambacher, and A. Erb, *Phys. Rev. B* **80**, 140510(R) (2009).
- ²¹Kensei Terashima, Takafumi Sato, Kosuke Nakayama, Toshiyuki Arakane, Takashi Takahashi, Maiko Kofu, and Kazuma Hirota, *Phys. Rev. B* **77**, 092501 (2008).
- ²²T. Yoshida, Seki Komiya, X. J. Zhou, K. Tanaka, A. Fujimori, Z. Hussain, Z.-X. Shen, Yoishi Ando, H. Eisaki, and S. Uchida, *Phys. Rev. B* **80**, 245113 (2009).
- ²³Aaron Bostwick, Jessica L. McChesney, Konstantin V. Emtsev, Thomas Seyller, Karsten Horn, Stephen D. Kevan, and Eli Rotenberg, *Phys. Rev. Lett.* **103**, 056404 (2009).
- ²⁴A. F. Santander-Syro, M. Ikeda, T. Yoshida, A. Fujimori, K. Ishizaka, M. Okawa, S. Shin, R. L. Greene, and N. Bontemps, *Phys. Rev. Lett.* **106**, 197002 (2011).